Effects of Nonrectangular Electrodes and Temperature in $LiNbO_3$ Based Optical Modulators

Khémiri Khéareddine*, Tahar Ezzedine and Houria Rezig

National Engineering School of Tunis. Laboratory SysCom, ENIT PB 37, Tunis 1002, Tunisia

Abstract: The effects of electrodes geometry and temperature on high frequency RF transmission characteristics are simulated versus $LiNbO_3$ layer thickness, inter-electrode gap, and optical waveguide parameters. On the other hand, we focused on the optimization of the electro-optic modulator parameters where the effective index plays an essential role in the evaluation of the bandwidth structure. Therefore, a theoretical analysis of the capacitance, the characteristic impedance and the effective index determine how to increase the bandwidth. The study of the variation of the effective index *versus* temperature shows a net drift, which affects the quality of transmission. Moreover, an approximate estimate of S-parameters shows the sensitivity of reflection and transmission ratios upon temperature.

The interaction optical-microwave is also analyzed using Laplace equation and Finite Element Method.

Keywords: Thermo-optic effect, electrode geometry, modulation bandwidth, electro-optic modulator, RF impedance and capacitance, effective index, S-parameters.

1- INTRODUCTION

Electro-optical modulators are widely used in external modulation integrated in high-speed transmission systems, compared to semiconductor-based homologues used in internal modulation whose speed is limited to 5Gb/sec. $LiNbO_3$ based modulators are compatible with wide bandwidth and weak dispersive optical fibers. The effective index of the optical device is a crucial parameter, which controls the bandwidth. The studied $LiNbO_3$ based structure is composed of two layered electrodes submitted to RF signal. Simultaneously, an optical stationary excitation is injected inside the waveguide. An electrical field is created within the waveguide. This field induces anisotropic changes in the light-waveguide index (permittivity) [1-3].

Several works studied the assumed rectangular electrodes. This geometry is theoretical and in the practical case, the section is somehow misshaped because of the growth process. Recent studies indicate that the conductor profile deeply affects the electrical characteristic of the microstrip [4-6].

Edge effects affect mainly the characteristic impedance, the capacitance and consequently the effective index controlling the bandwidth [6].

We have also observed a thermo optical effect through a thermal induced change in refractive index [7]. The recorded thermal originated phase shift is superposed on that induced by the electrical field.

These effects produce a change in the operating state of the device and, therefore, induce a distortion in the device behavior.

*Address correspondence to this author at the National Engineering School of Tunis. Laboratory SysCom, ENIT PB 37, Tunis 1002, Tunisia; Tel: 00216 71 875 475; Fax: 00216 71 872 729; E-mail: khemiri.khe@voila.fr

The theoretical study of the device starting from Maxwell equations assumes the quasi-TEM conditions because:

i) the device size is smaller than the wavelength currently used,

ii) the device geometry is invariant according to the longitudinal axis of wave propagating inside the waveguide [8, 9] .

The static field is solved with the Laplace equation in all the regions of the structure with the suitable boundary conditions. This problem has been solved using the finite element method. This method is often successfully used in simulating opto-microwave devices.

We have chosen the triangular shape, which seems to give good results with low dimension matrices.

In this work, we take advantage from the use of Comsol Multiphysics™ (FEMLAB 3.1).

2- THEORY

The optical wave propagating inside the waveguide follows the Helmholtz equation (1):

$$\nabla^2 E(x,y,z) + k_0^2 n^2 E(x,y,z) = 0 \quad (1)$$

If Oz is the axis of propagation with propagation constant β, the Optical Field (OF) in (xoy) plan is the solution of the following expression [10, 1]:

$$\left(\frac{\partial^2}{\partial x^2} + \frac{\partial^2}{\partial y^2}\right) E(x,y) + (k_0^2 n^2 - \beta^2) E(x,y) = 0$$

However, according to Ox axis, this OF expression can be extracted from (2):

$$\frac{\partial^2}{\partial x^2} E(x) + (k_0^2 n^2 - \beta^2) E(x) = 0 \quad (2)$$

1874-3285/10

In order to study the Optical-Microwave interaction, we use a quasi steady state approach giving us the electric field distribution Ē (radiofrequency wave) inside the structure. As it has been said, this field is applied on the electrodes in order to monitor permittivity changes in the optical waveguide structure. Such a monitoring is operated through the electric field which is itself controlled by the biasing voltage **Φ**, according to Laplace equation (3).

$$\vec{E}(x,y) = -\nabla\Phi(x,y) \ , \ \nabla(\bar{\bar{\varepsilon}}.\nabla\Phi) = 0 \quad (3)$$

Ē is the electric field and $\bar{\bar{\varepsilon}}$ is the permittive tensor [2].

Solving this system leads to the distribution of the electric field over the inter electrodes embedded region of the waveguide (Fig. **1**).

Nevertheless, the evaluation of the bandwidth needs to determine the effective permittivity ε_{eff} *versus* the capacitance and impedance parameters [11, 12]:

$$\Delta f = \frac{2C}{\pi\left|N_0 - N_m\right|L} \quad (4)$$

Where: $N_m = \sqrt{\varepsilon_{eff}}$, $\varepsilon_{eff} = \frac{C}{C_0}$

C_0 is vacuum capacitance and C is the capacitance in the waveguide structure [13, 14].

N_0: the effective refractive optical index (related to the optical wave); while N_m is the effective index (related to the electrical modulating wave); L: length of electrodes.

Impedance and capacitance are deduced from the following relationship (5):

$$Z_c = \frac{1}{c\sqrt{C\ C_0}} \ ; \ C = \frac{Q}{\Delta V} \quad (5)$$

Where c: light speed in vacuum, Q: electrical charge induced in the electrode according to the following relationship (6):

$$Q = \int \vec{D}\ \vec{n}\, ds \quad (6)$$

Where $\vec{D}$ is the electrical displacement vector.

In fact, the effective index must be lowered through the optimization of the impedance and capacitance of the structure.

3. EVALUATION OF STRUCTURE PARAMETERS

3.1. Rectangular Electrodes Case

To solve a particular electrostatic problem and find the Distribution of Electric field in the optical waveguide region distribution, it is necessary to specify the structure geometry (Fig. **1**) and the electrostatic properties and boundary condition. These conditions are essentially of two types: Dirichlet or Neumann.

In the first type, a potential is imposed on the surface of electrode *V* (in our case a potential is imposed to one electrode).

The second type of condition sets the electrical displacement vector. $\vec{D}$ on a boundary as,

$$n\ (D_1 - D_2) = 0 \quad (7)$$

where n stands of the surface normal, *D* is definided as

$$D = \varepsilon_0 \varepsilon_r E \quad (8)$$

and the electric field is obtained from the gradient of V

$$E = -\ \nabla\ V \quad (9)$$

Fig. (**1**) shows the analyzed structure. It consists of a buffer 0.2µm thick layer of silica grown on $LiNbO_3$ substrate. The length of the waveguide is 5 cm.

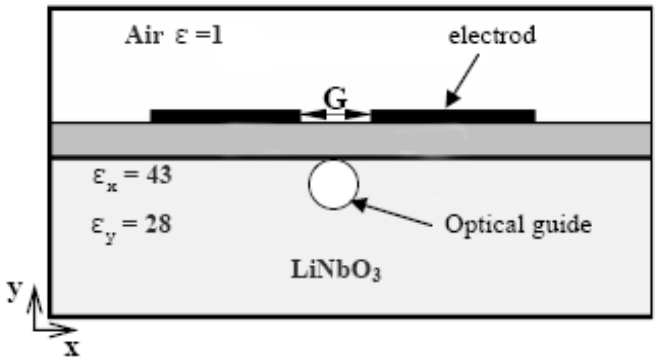

Fig. (1). $LiNbO_3$ based electro optical Structure.

A couple of electrodes are assumed to be rectangular and perfect conductors (4µm thick and 5µm wide). G is the inter-electrodes length gap.

Whereas, the maximum element size scaling factor is 0.55, the mesh curvature factor is 0.25 and the mesh curvature cut off is 0.0005 by following the number of elements is 9966.

A previous study* allowed the determination of the electric field shape in the optical waveguide region (Fig. **2**). In this region, we try to enhance the electric field intensity in order to increase the variation amplitude of the effective index.

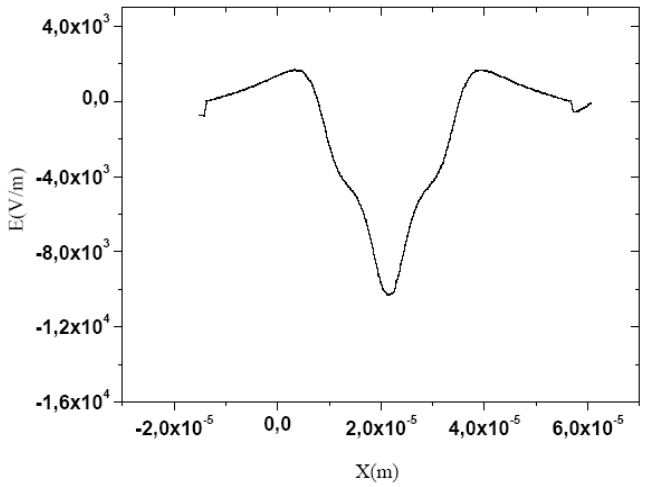

Fig. (2). Distribution of Electric field in the optical waveguide region.

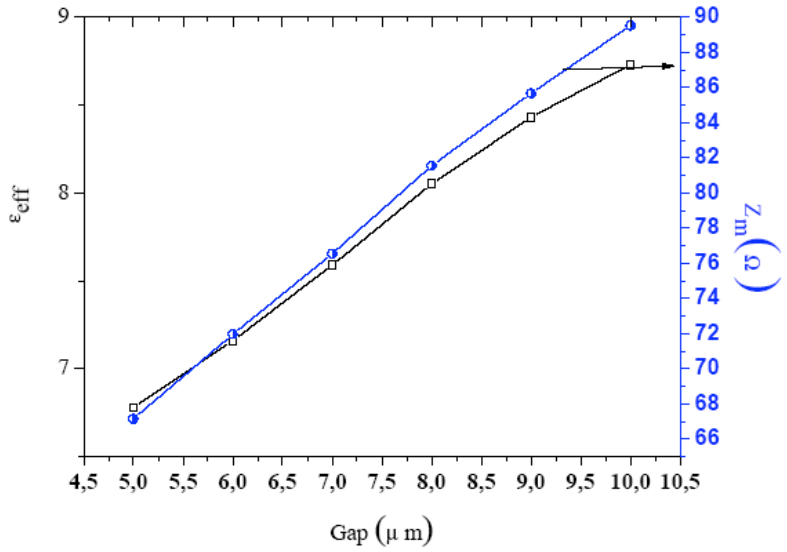

Fig. (3). Effective permittivity and impedance behaviours *versus* length gap.

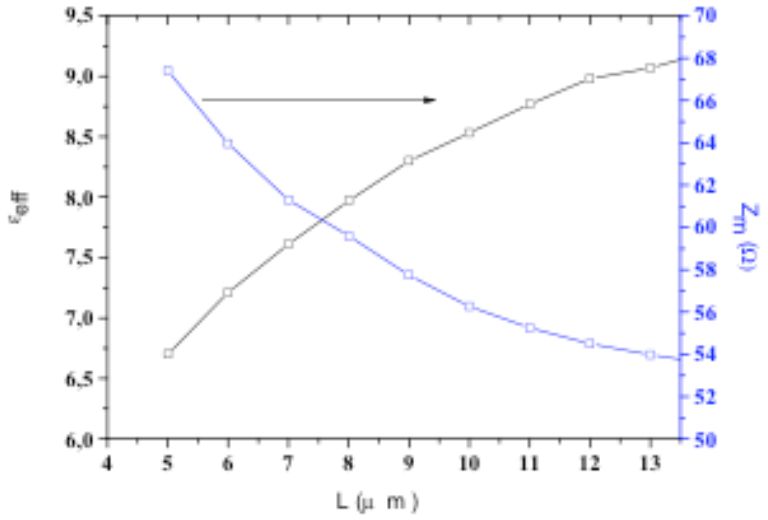

Fig. (4). Effective permittivity and impedance behaviour *versus* electrode width.

As it is has been mentioned above, the bandwidth is a key performance parameter in an electro-optical modulator. The increase of this bandwidth depends mainly on the effective index (near 2.2).

We notice that the effective index behaves almost linearly with the gap (Fig. **3**), while it increases with the electrode width before reaching a saturation effect (Fig. **4**).

Moreover, one should work in optimal energy transmission conditions so the characteristic impedance has to be the closest to 50Ω.

3.2. Case on Non-Rectangular Electrode

We have simulated several mis-shaped electrodes with different oblique corners (Fig. **5**), which are assumed to be originated from growth process defects (edge effects, uncontrolled temperature, asymmetric system) [15]. We have used the results of the former section*, changed the electrodes thickness (T) and adopted two different oblique corner angles $\alpha = 90°$ (rectangular) and $\alpha = 60°$.

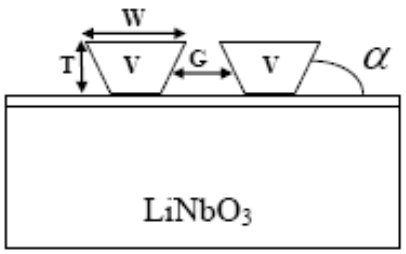

Fig. (5). $LiNbO_3$ based electro optical non-rectangular Structure.

*K. Khéareddine *et al.* ''Evaluation des performances d'un modulateur a électrode non rectangulaire lors d'une transmission 40Gbit/s''. Congrès Méditerranéen des Télécommunications Tanger, Morocco 14-15 Mars 2008.

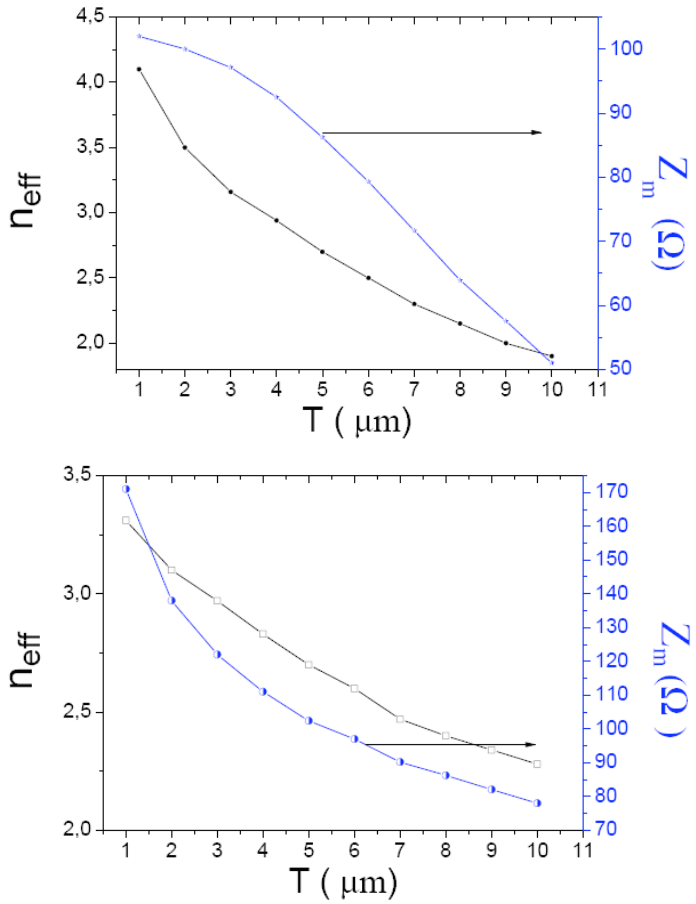

Fig. (6). Effective index and impedance behaviours for different electrode glazing angles. (**a**) 60°, (**b**) 90°.

The characteristic impedance of the electrode and the effective dielectric constant for the electric wave-guide on the electrode are two important parameters in the design of electro-optical devices. The broadband modulation may be achieved by decreasing the difference between N_0 and N_m. So when we decrease the index of N_m we decrease the effective dielectric constant ε_{eff}.

In order to control the impedance, and the effective dielectric constant ε_{eff}, we have to study the effect of the electrodes thickness by fixing the separation gap G for a value of 5 µm.

It comes out that the case of 60° seems to give better results of effective index and impedance behaviors n_{eff} near 2.2 And Z_c around 50 Ω, Fig. (**6**) (case a).

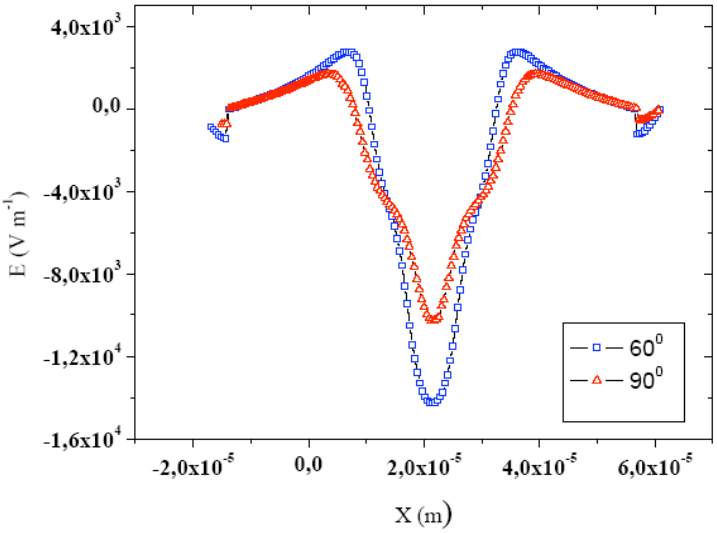

Fig. (7). Electric Field Variation versus electrode width for two different angles.

We also present the variation of the field distribution in each case with the thickness being fixed at T = 9µm. Again, the 60° case gives the best result for a similar shape of the general behaviour (Fig. **7**).

4. TEMPERATURE EFFECTS ON MODULATOR PARAMETERS

Given the specific heat of water (4,180 KJoule/kg.K (at 0°C, normal pressure conditions), the estimation of the thermo-optical effect can be studied through (10) heat transfer equations according to the conduction mode [16-19]:

$$\rho C \frac{\partial T}{\partial t} + \nabla.(-K\ \nabla T) = Q \qquad (10)$$

Where T is Kelvin temperature [K], Q is the heat emitted by the heat source [W/m^3], ρ is the massic density [Kg/m^3], C is heat capacity [J/Kg.K] and K is heat conductivity of the media [W/m.K].

The surface specific heat flux is given by Fourier law (11):

$$q = - K\ \nabla T\ [W/m^2] \qquad (11)$$

On the other hand, the variation of the ordinary and extraordinary indices of $LiNbO_3$ *versus* temperature can be written as follows (12) and (13):

$$\frac{dn_0}{dT} = -0.9 + 3\times10^{-3} T\ (10^{-5}\ K^{-1}) \qquad (12)$$

$$\frac{dn_e}{dT} = -2.6 + 19.8\times10^{-3} T\ (10^{-5}\ K^{-1}) \qquad (13)$$

The effective index resulting from the temperature effect is:

$$n'_{eff(LiNbO_3)} = n_{eff(LiNbO_3)} + \Delta n_{eff(LiNbO_3)} \qquad (14)$$

4.1. Field and Effective Index Behaviors *versus* Temperature

Intrinsic or extrinsic originated temperature effects induce drastic changes in modulator parameters namely the effective index as it is shown in Fig. (**8**).

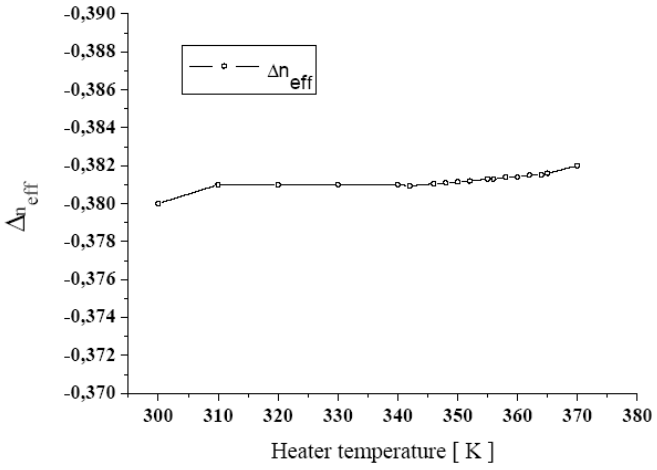

Fig. (8). Variation of the effective index *versus* temperature.

This will induce a change in the electric field inside the waveguide. This field decreases with temperature. Fig. (**9a**) shows the variation of the electric field versus the width of the structure at different temperatures. Such a decrease lowers the sensitivity of the optical waveguide to the radiofrequency excitations applied on the electrodes. Fig. (**9b**) zooms on the central region in order to improve the readability of the curve.

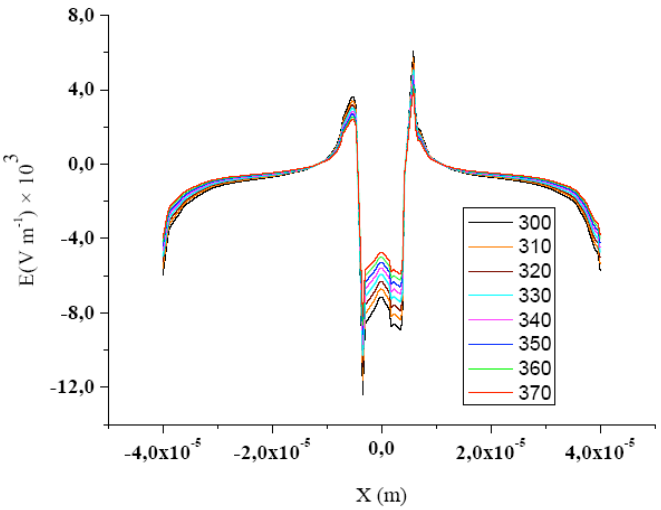

Fig. (9a). Temperature effect on the electrical field behaviour *versus* structure width.

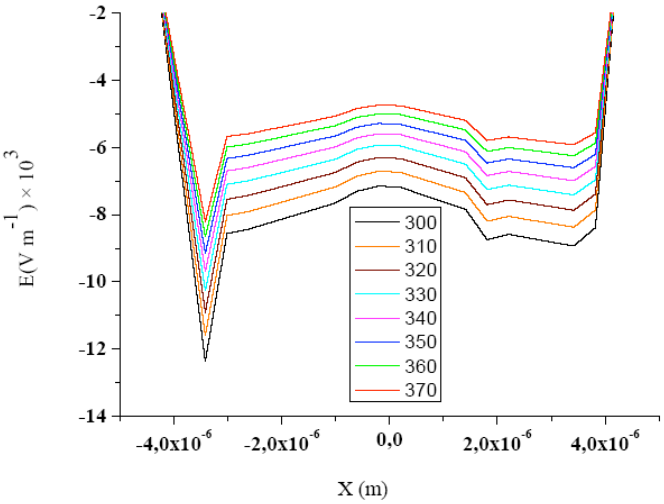

Fig. (9b). Scale magnification of the central region of Fig. (**9a**).

One can observe a noticeable decrease of the field distribution while the temperature increases. Then, the inter electrodes region of the waveguide will be insensitive to the electric field and might produce a dysfunction of the modulator.

However, it has been reported that the thermo effect has been used to realize some functions like: Digital Optical Switch Filter/Multiplexer [20-22].

4.2. Calculation of the Variation of S Parameters *versus* Temperature Change

In general, it is useful to estimate S parameters of the structure [23]. Thus, Reflection and Transmission coeffi-

cients respectively S_{11} and S_{21} are, then, given by equations (15) and (16):

$$S_{11} = \frac{\int_{port1} ((E_z - E_{0z}).E_{0z})\, dA}{\int_{port1} E_{0z}^2 dA} \quad (15)$$

$$S_{21} = \frac{\int_{port2} (E_z.E_{0z})\, dA}{\int_{port2} E_{0z}^2 dA} \quad (16)$$

E_z is the total field and E_{0z} the incident field. Fig. (**10**) and Fig. (**11**) show S_{11} and S_{21} without and with temperature change respectively.

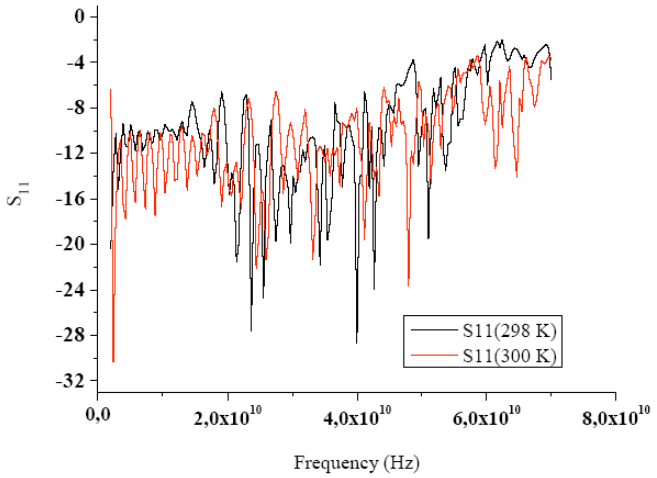

Fig. (10). Reflection coefficient S_{11} plotted for two different temperatures.

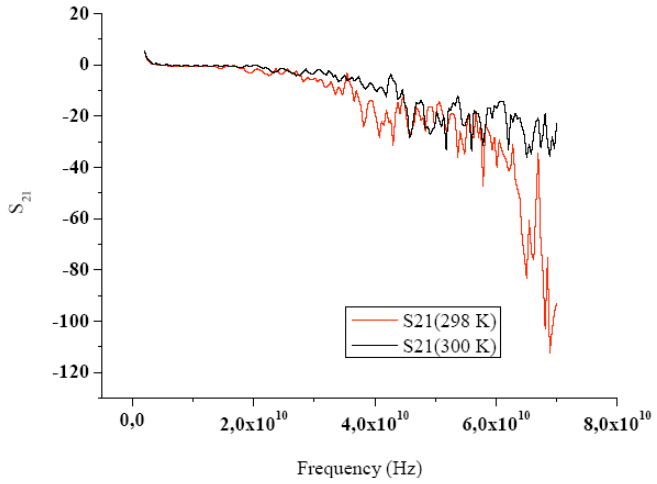

Fig. (11). Transmission coefficient S_{21} plotted for two different temperatures.

One can notice that, for the explored temperature range, while the reflection coefficient is almost invariant, we observe a noticeable decrease of the transmission coefficient at the highest frequencies. This could be explained by the volume effect of the temperature on the effective index, which is less obvious on reflection coefficient.

CONCLUSION

The effects of rectangular, non-rectangular electrodes and temperature in $LiNbO_3$ Optical Modulators were studied by using the finite element method. We took into account all geometrical and material parameters, and the multi-physics integration of both optical and thermal investigations. The classical wave and Laplace equations were used to study the effect of a microwave field on an optical co-propagating in a travelling-wave modulator structure in the cross section. The characteristic impedance, the capacitance and the effective permittivity are obtained from the potential and the field distributions. We have simulated several mis-shaped electrodes with different oblique corners which are assumed to be originated from growth process defects (edge effects, uncontrolled temperature, asymmetric system...). It comes out that the case of oblique electrode seems to give better results of effective index and impedance behaviors. Nevertheless, the evaluation of the bandwidth needs to determine the effective permittivity *versus* capacitance and impedance parameters. We have also simulated the variation of the electrical field in the inter electrode region with a temperature derive. The field decreases with temperature. Such a decrease lowers the sensitivity of the optical wave-guide to the radiofrequency excitations applied on the elec-trodes. However, the temperature derive can be performed with other materials, including for example polymers, and can be applied to the design of devices employing this thermo-optic effect, such as optical switches and ring resonators.

REFERENCES

[1] Kenji K. Spectral-Domain analysis of coplanar waveguide travelling-wave electrodes and their applications to Ti:LiNbO, mach-zehnder optical modulators. IEEE Trans Micro Theory Tech 1991; 39(9): 1595-601.

[2] Rod CA. Waveguide electrooptic modulators. IEEE Trans Micro Theory Tech 1982; 30(8): 1121-37.

[3] Darío F, James NE. Coupled-Mode znalysis of an electrooptic frequency shifter. IEEE J Quant Elect 2003; 39(2): 358-63.

[4] Naghski DH, Boyd JT, Jackson HE, *et al*. Latess. An integrated photonic mach-zehnder interferometer with no electrodes for sensing electric fields. IEEE J Light Tech 2004; 12(6): 1092-98.

[5] Li G, Yu KL. Optical intensity modulators for digital and analog applications. J Light Tech 2003; 21(9): 2010-30.

[6] H. Jin. General analysis of electrodes in integrated-optics electrooptic devices. IEEE J Quant Elect 1991; 27(2): 243-51.

[7] Suntak P, Jung JJ, Jung YD, *et al*. Thermal stability enhancement of electrooptic polymer modulator. IEEE Photonics Tech Lett 2004; 16(1): 93-5.

[8] Rahman BM. Finite-element solution of integrated optical waveguides. IEEE J Light Tech 1984; (26): 82-8.

[9] Keen AG, Wale MJ, Sobhy MI. Quasi-Static analysis of electrooptic modulators by the method of lines. IEEE J Light Tech 1990; 8(1); 42-50.

[10] Wiley J, Sons Inc. Introduction to optical waveguide analysis copyright. 2001.

[11] Mahmoud MT, Sebastien G, Samir M, *et al*. Time-domain optical response of an electrooptic modulator using fdtd. IEEE Trans Micro Theory Tech 2001; 49(12); 2276-81.

[12] Azizur BM, Haxha V, Haxha S, *et al*. Design optimization of polymer electrooptic modulators. IEEE J Light Tech 2006; 24(9): 3506-13.

[13] Marcuse D. Optimal electrode design for integrated optics modulator. IEEE J Quan Elect 1982; 18(3): 393-98.

[14] Ding YC, Jamie DP. Analysis and design optimization of electrooptic interferometric modulators for microphotonics applications. IEEE J Light Tech 2006; 24(6): 2340-46.

[15] Fang LL, Ruey-Beei W. Analysis of coplanar-waveguide discontinuities with finite-metallization thickness and nonrectangular edge profile. IEEE Trans Micro Theory Tech 1997; 4(5): 19-12.

[16] Francesca M, Francesco D, Vittorio MN. Multiphysics investigation of thermo-optic effect in silicon-on-insulator waveguide arrays. Excerpt from the Proceedings of the COMSOL Users Conference 2006; Milano.

[17] Moretti L, Iodice M, Della Corte FG, *et al*. Temperature dependence of the thermo-optic coefficient of lithium niobate, from 300 to 515 k in the visible and infrared regions. J App Phys 2005; 9(8): 36-101.

[18] Saadon H. L, Théofanous N, Aillerie M, *et al*. Thermo-optic effects in electro-optic crystals used in an intensity-modulation system. Application in $LiTaO_3$. Las and Opt / Appl Phys 2006; 8(3): 609-17.

[19] Aillerie1 M, Théofanous N, Saadon. HL. Thermo-optic effects in an electro-optic modulation system. NAMES 2007, 3rd France-Russia Seminar Metz, (7-9).

[20] Passaro VMN, Magno. F, Tsarev A. Investigation of thermo-optic effect and multireflector tunable filter/multiplexer in soi waveguides. Opt Exp 2005; 1(3): 3429-37.

[21] Iodice M. Thermo-optic static and dynamic analysis of a digital optical switch based on amorphous silicon waveguide. Opt Exp 2006; 14: 5266-78.

[22] Mikko H, Markku K, Timo A, *et al*. Sub- switching time in silicon-on-insulator mach–zehnder thermooptic switch. IEEE Photonics Technol Lett 2004; 1(6): 2039-41.

[23] Woo KK, Woo-Seok Y, Han-Young L. Effects of parasitic modes in high-speed $LinbO_3$ optical modulators. Opt Exp 2004; 1(2): 12-14.

Received: August 15, 2010 Revised: October 18, 2010 Accepted: October 20, 2010